Persistent current and Wigner localization in a one-dimensional quantum ring

Marc Siegmund*
Lehrstuhl für Theoretische Festkörperphysik, Universität Erlangen-Nürnberg,
Staudtstrasse 7 B2, D-91058 Erlangen, Germany
(Dated: April 17, 2007)

We use Density Functional Theory to study the localization of interacting spinless electrons on a one-dimensional quantum ring when the system undergoes a Wigner crystal transition at low electron densities. The resulting crystalline state is pinned by a weak Gaussian potential. As a criterion for the localization of such a correlated many particle state we suggest the persistent current in the ring as a function of the one-dimensional Wigner-Seitz radius r_S. It is shown that for vanishing impurity potential strength the persistent current is constant up to a critical value r_S^c and decreases exponentially for $r_S > r_S^c$. We interpret this behaviour as the formation of a Wigner crystal phase at $r_S^c \approx 2.05$. This result is compared to the critical value of r_S obtained by using the curvature of the ground state energy with respect to the boundary conditions as a localization criterion.

I. INTRODUCTION

In the last few years, the experimental realization of very narrow two-dimensional quantum rings became possible[1,2]. In such systems only a few transverse states are occupied. By increasing the curvature of the confining potential the system can finally be made effectively one-dimensional. The number of electrons in such systems can be controlled by means of gate electrodes. Expermiental studies of rings with only one or two electrons were reported by Lorke *et al.*[3] The possibility to vary the number of particles from very few to several hundreds enables experimentalists to tune the electron-electron interaction in these rings. One of the most strinking consequences of electron interaction is the formation of a Wigner crystal[4], a many-body state with electrons localized at discrete lattice sites. However, due to the strong fluctuations in one dimension[5] the stability of such a crystalline phase has been a long-debated subject and it could be shown only in the nineties that an arbitrarly weak pinning potential indeed stabilizes the one-dimensional Wigner crystal[6].

From a theoretical point of view one question is how to measure the localization of such a correlated many body state. Several criteria have been suggested to distinguish between a localized and a delocalized state like the inverse participation number[7] or the curvature of the ground state energy[8]. However, to our best knowledge the electrons' ability to carry an electric current - which is the most direct localization criterion has not yet been explored. In this work we concentrate on the persistent current in a one-dimensional quantum ring penetrated by a magnetic flux and study its dependence on the strength of the electronic interactions.

This paper is organized as follows. In section 2 we discuss three different localization criteria including a persistent current in a quantum ring as the most direct one. In section 3 we briefly discuss the one-dimensional Wigner crystal and its stability despite the strong fluctuations in one dimensional systems. In section 4 we introduce our model and the computational method we used to obtain the persistent current as a function of r_S. The numerical resoluts for $j(r_S)$ are discussed in section 5. A conclusion is drawn in section 6.

II. LOCALIZATION CRITERIA

A. Inverse participation number

The localization of a single-particle state may be assessed qualitatively as a "concentration" of a single-particle wave function $\varphi(\vec{r})$ in a certain region of space. For a quantitative assessment one may consider the second moment of the probability distribution rather than the wave function directly. This quantity is called an inverse participation number[7] and is defined as

$$P^{-1} = \frac{\int d^3r\, |\varphi(\vec{r})|^4}{\left[\int d^3r\, |\varphi(\vec{r})|^2\right]^2}\,. \tag{1}$$

To illustrate the meaning of this expression consider the ground state of a particle of mass m in a harmonic potential with a frequency ω. The typical length scale of this system is given by $a = \sqrt{\frac{\hbar}{m\omega}}$. Using this we find for the wave function

$$\varphi(x) = \left(\frac{1}{\pi a^2}\right)^{1/4} \exp\left(-\frac{x^2}{2a^2}\right) \tag{2}$$

and hence for the inverse participation number

$$P^{-1} = \frac{1}{\sqrt{2\pi}a}\,. \tag{3}$$

Now if the system gets more localized (the spread of the wave function decreases, i.e. a decreases) P^{-1} increases and if the system gets more delocalized P^{-1} decreases.

However, the definition (1) of the inverse participation number given in terms of single-particle wave functions is not suitable for a many-body state. Alternatively to (1), one may define the inverse participation number for

a single-particle system using the single-particle probability density $\rho(\vec{r})$

$$P^{-1} = \frac{\int d^3r\, |\rho(\vec{r})|^2}{\left[\int d^3r\, \rho(\vec{r})\right]^2}\,. \tag{4}$$

This definition allows a generalization to a many-particle state by replacing the single-particle probability density by the total density of the many-body system[7]. However, this so called generalized participation number will not be used in the rest of this work and we concentrate instead on two localization criteria which are more rigorously justified for the many-particle case.

B. Curvature of the ground state energy

Rather than directly looking at the wave function one may explore the sensitivity of the ground state energy to the boundary conditions as a localization criterion. Roughly speaking the localized state does not feel any change of the boundary conditions and thus the ground state energy does not change, whereas the response of a delocalized state is finite irrespective of how large the system is.

In fact, it has been shown that the curvature of the ground state energy with respect to the boundary conditions can be used to distinguish between a localized and a delocalized system[8]. This quantity is related to the charge stiffness D in the Drude model of the conductivity. In the thermodynamic limit one finds for an insulator $D \to 0$, whereas D approaches a finite, nonzero value for a metal[7].

In contrast to the above mentioned inverse participation number, the curvature of the ground state energy can be directly used in a many-body case. It is especially suitable for density functional calculations since the ground state energy is in principle given exactly by static DFT.

C. Persistent current as a localization criterion

The most direct feature that distinguishes a localized and a delocalized many particle state is the ability of a state to carry the current. In this work we concentrate on the persistent current in a ring geometry rather than on a transport current since the persistent current is a ground-state property and hence may be obtained by the static DFT. This is by far easier than computing a dissipative current which involves excitations of the many particle system.

To illustrate why the persistent current may be used as a localization criterion consider first a clean one-dimensional quantum ring i.e. a system without impurities (figure 1). In the absence of the electron-electron interaction the total persistent current is obtained as a sum of currents carried by the individual particles. When the electron-electron interaction is switched on the system rotates as a whole and the current remains unchanged[20].

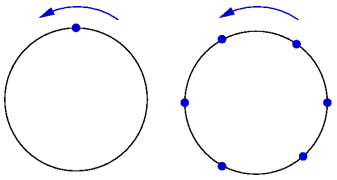

FIG. 1: Persistent current in clean sample. Left: single-particle contribution to the current in a non-interacting system. Right: rigid rotation of the correlated system.

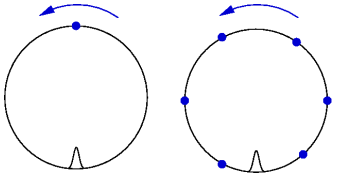

FIG. 2: Persistent current in sample with Gaussian impurity. Left: single-particle contribution to the current in a non-interacting system dictated by single-particle tunneling. Right: tunneling of the correlated system as a whole.

This behaviour changes drastically in the presence of an impurity potential (figure 2). For a system of non-interacting particles the persistent current is still the sum of the individual single-particle contributions and is hence dictated by single-electron tunneling through the impurity. In contrast to this, a correlated state has to tunnel as a whole which significantly reduces the tunneling probability and hence the persistent current.

III. ONE-DIMENSIONAL WIGNER CRYSTAL

Consider a one-dimensional electron gas with the dispersion relation $\varepsilon(k) = \frac{\hbar^2}{2m^*}k^2$. The kinetic energy per particle is given by

$$\frac{T}{N} = \frac{L}{2\pi N}\int_{-k_\mathrm{F}}^{k_\mathrm{F}} \frac{\hbar^2 k^2}{2m^*} dk \propto n^2 \tag{5}$$

whereas the Coulomb energy per particle is proportional to the distance between the particles and hence to the density:

$$\frac{V}{N} \propto \frac{1}{d} \propto n\,. \tag{6}$$

Thus, at high densities, the kinetic contribution dominates the total energy of the system. Therefore the most favourable state of the system is a deloclaized, free electron gas-like one. In contrast, at low densities the Coulomb repulsion dominates the total energy which tries to keep electrons apart at possibly large separations. The most favourable configuration in this limit is clearly a regular arrangement of electrons at equidistant lattice sites.

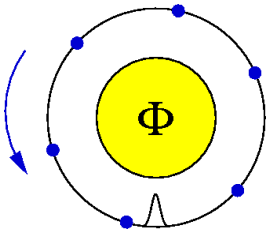

FIG. 3: Illustration of the model used for the calculation: a one-dimensional system with periodic boundary conditions containg N electrons. A magnetic flux Φ penetrates the ring and induces a persistent current. The Wigner crystal phase is pinned by a Gaussian impurity potential.

However, this simple picture is complicated by the quantum mechanical zero point oscillations of the normal modes of this chain of localized particles which lead to fluctuating displacements of the electrons. In fact it can be shown that in one and two dimensions no stable crystalline order exits[5]. However, in one dimension the Wigner crystal phase is stabilized by an arbitrarily weak pinning potential which suppresses the long wavelength (soft) modes of the fluctuation field[6].

IV. MODEL AND METHOD

A. Model

We model the one-dimensional quantum ring as a linear system of length L with periodic boundary conditions containing $N = 10$ spinless electrons (see figure 3).

A magnetic flux Φ penetrates the ring and induces a persistent current. In the region where the electrons move the corresponding vector potential is given by

$$\vec{A} = \frac{\Phi}{L}\vec{e}_\varphi \tag{7}$$

where $\vec{e}_\varphi$ is the polar unit vector i.e. pointing along the circumference of the ring. This vector potential is chosen such that the electrons move in a region with zero magnetic field and the only influence of the vector potential on the wave function is that it acquires an additional phase depending on the number of flux quanta penetrating the ring.

Additionally, a Gaussian impurity potential of the strength V_0 and width a

$$V_{\text{imp}}(x) = V_0 \exp\left(-\frac{x^2}{a^2}\right) \tag{8}$$

with x being the coordinate along the ring is placed in the system. This barrier is required both for pinning the Wigner crystal phase and to ensure the convergence of the numerical computations.

Including these external contributions the Hamiltonian of the system is given by

$$\hat{H} = \sum_{k=1}^{N}\left[\frac{\hbar^2}{2m_0^*}\left(-i\frac{d}{dx_k} - \frac{2\pi}{L}\frac{\Phi}{\Phi_0}\right) + V_{\text{imp}}(x_k)\right] + \frac{1}{2}\sum_{k\neq l}\frac{e^2}{|x_k - x_l|} \tag{9}$$

where m_0^* is the effective electron mass and $\Phi_0 = \frac{h}{e}$ is the elementary flux quantum.

The system will undergo a Wigner transition from a delocalized electron gas like state to a localized crystalline state when the Coulomb energy V_{c} exceeds the kinetic energy T. The ratio of these energies is given by the one-dimensional Wigner-Seitz radius

$$r_{\text{S}} = \frac{1}{2}\frac{L}{N}\frac{1}{a_{\text{B}}} \propto \frac{\langle V_{\text{c}}\rangle}{\langle T\rangle} \tag{10}$$

which measures the average distance between the particles in units of the Bohr radius

$$a_{\text{B}} = \frac{\epsilon\hbar^2}{m_0^* e^2}\,. \tag{11}$$

Using parameters for GaAs (dielectric constant $\epsilon = 12.5$ and effective electron mass $m_0^* = 0.0665 m_{\text{e}}$) we find $a_{\text{B}} = 9.95 \cdot 10^{-9}\text{m}$.

We expect that the system will be in a delocalized phase for $r_{\text{S}} \ll 1$ and in a localized phase for $r_{\text{S}} \gg 1$. Experimentally, the parameter r_{S} is controlled by the number of electrons in the system, i.e. the density. Yet the density is not the most conveniant parameter to change in the theoretical calculations, since changing the number of electrons changes the Fermi level. This, of course, changes the persistent current even in a non-interacting system. Therefore, the most convenient parameter to change is the effective mass of the electrons.

First, we replace the true effective electron mass m_0^* in the kinetic energy contribution to the Hamiltonian by a fictitious one m^*. Yet, there is a second energy ratio that has to be considered. In order to guarantee that the persistent current of a single particle is not affected by changing the effective electron mass, the Gaussian potential barrier V_{imp} has to be renormalized according to

$$V_0 \to V_0^* = V_0\frac{m_0^*}{m^*}\,. \tag{12}$$

Finally, all observables, especially the persistent current, have to be calculated using the true effective electron mass m_0^*. This procedure guarantees that the persistent current of a system of non-interacting electrons is independent of r_{S}. Hence any change in the persistent current as r_{S} is varied we observe in our calculations is purely due to the electron electron interaction.

B. Density Functional Theory

For actually solving the interacting many body problem in the presence of a magnetic flux and an impurity

potential we use Density Functional Theory (DFT). The fundamental statement in static DFT is the so-called Hohenberg-Kohn theorem[9] which establishes a one-to-one correspondence between the density and the external potential in an interacting many body system. Therefore, all observables may be expressed as functionals of the electronic density alone.

For practical purposes, however, the Kohn-Sham construction[10] is of special importance. It provides an in principle exact method for calculating the density of the fully interacting, inhomogeneous system using an artificial non-interacting system in an effective potential. The Hamiltonian $\hat{H}_{\mathrm{KS}}$ of this system is given by

$$\hat{H}_{\mathrm{KS}} = \frac{1}{2m^*}\left(-i\hbar\frac{d}{dx} - eA\right)^2 + V_{\mathrm{imp}} + V_{\mathrm{H}} + V_{\mathrm{xc}} \quad (13)$$

where V_{H} is the ordinary electrostatic Hartree potential and V_{xc} is the exchange-correlation potential which contains all many-body quantum effects. Both the Hartree- and the xc-potential are functionals of the density $n(x)$. Therefore, the resulting Kohn-Sham equations

$$\hat{H}_{\mathrm{KS}}\varphi_i(x) = \varepsilon_i\varphi_{\mathrm{i}}(x) \qquad n(x) = \sum_i |\varphi_i(x)|^2 \quad (14)$$

have to be solved self-consistently.

Since our goal is to calculate the persistent current directly from the Kohn-Sham orbitals φ_i the question arises whether we have to use Current Density Functional Theory (CDFT)[11] instead of ordinary DFT. In contrast to DFT where the basic variable is the density alone, CDFT includes the (paramagentic) current density $\vec{j}_{\mathrm{p}}$ as a second basic variable. This means that the KS orbitals of CDFT are guaranteed to reproduce in principle the exact current density as well as the exact density whereas the KS orbitals of ordinary DFT merely reproduce the exact density but not the current density. From a practical point of view, the only difference between the KS systems in DFT and CDFT is that in addition to the scalar xc-potential an exchange-correlation vector potential enters the KS Hamiltonian in CDFT due to the fact that now all observables are functionals of the density and the paramagnetic current density[21].

Clearly, the ground state energy has to be gauge invariant while the paramagnetic current density changes under a gauge transformation $\vec{A} \to \vec{A}' = \vec{A} - \nabla\Lambda$ according to

$$\vec{j}'_{\mathrm{p}}(\vec{r}) = \vec{j}_{\mathrm{p}}(\vec{r}) + \frac{e}{m}n(\vec{r})\nabla\Lambda(\vec{r})\,. \quad (15)$$

This requires that the xc-energy functional does not depend directly on $\vec{j}_{\mathrm{p}}$ but on the vorticity $\vec{v} = \nabla \times \frac{\vec{j}_{\mathrm{p}}}{n}$.[11] It can be shown that a particularly simple approximation of the xc-energy functional is local in the vorticity and leads to an xc vector potential of the form

$$\vec{A}_{\mathrm{xc}} \propto \frac{1}{n}\nabla \times \left(\nabla \times \frac{\vec{j}_{\mathrm{p}}}{n}\right)\,.^{11} \quad (16)$$

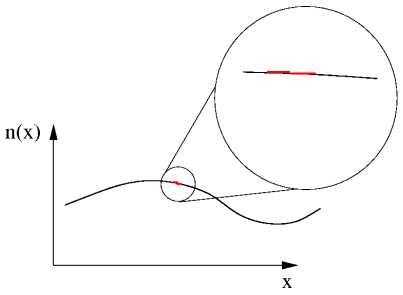

FIG. 4: Illustration of the Local Density Approximation. An inhomogeneous system (black curve) is considered to be locally homogeneous (red lines).

For strictly one-dimensional system this expression vanishes. Physically this may be traced back to the fact that $\vec{A}_{\mathrm{xc}}$ describes a distortion of the wavefunction in the presence of currents[11]. In one dimension this distortion is purely longitudinal and hence described by the scalar xc-potential. Therefore in our specific case of a strictly one-dimensional quantum ring CDFT reduces to ordinary DFT.

Still, an approximate expression for the xc-potential is needed while the Hartree potential is known exactly. A widely used form is the so-called Local Density Approximation (LDA)[10] where the inhomogeneous system is considered to be locally homogeneous (see figure 4). The xc-energy of the inhomogeneous system is then given as an integral of the contributions of the locally homogeneous parts of the system

$$E_{\mathrm{xc}}^{\mathrm{LDA}}[n] = \int dx\, n(x) e_{\mathrm{xc}}(n(x)) \quad (17)$$

with the xc-energy per particle $e_{\mathrm{xc}}(n)$ of a homogeneous electron gas with density n. This approximation is valid if the length scale of the density variation l is much larger than the typical length scale in the system which is given by k_{F}^{-1}: $k_{\mathrm{F}}l \gg 1$.

However, a better local approximation for the exchange energy is availabe which will be used in this work, namely the Optimized Effective Potential method (OEP)[12]. The idea behind the OEP is to minimize the exchange energy functional not with respect to the density directly but with respect to the Kohn-Sham wavefunctions. This results in an integral equation for the exchange potential which in general cannot be solved. However, with the KLI approximation[13,14] a very good approximate solution is avilable. In contrast to the LDA potential the OEP potential has the correct $\frac{1}{r}$-dependence for large distances ($r \to \infty$) and in fact, the OEP potential is the best local approximation for the exchange potential.

C. Computational method

For the numerical solution of the Kohn-Sham equations, a representation of the wavefunctions has to be

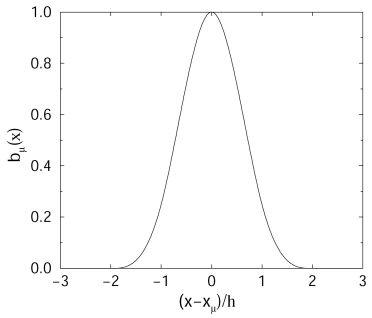

FIG. 5: A single spline function, taken from Ref. 7

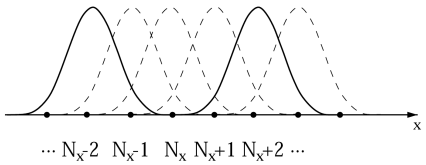

FIG. 6: Overlap of adjacent spline functions, taken from Ref. 7

chosen. A widely used method is to expand the wavefunctions in a plane-wave basis. However, it would require a large number of plane waves to describe a localized state. Therefore it is more suitable to use a set of localized functions as a basis. The basis functions chosen in this work are spline functions[7] which are piecewise defined real third order polynomials:

$$b_\nu(x) = \begin{cases} \frac{1}{4}\left(2+\frac{x-x_\nu}{h}\right)^3 & : \quad -2 < \frac{x-x_\nu}{h} \le -1 \\ 1-\frac{3}{2}\left(\frac{x-x_\nu}{h}\right)^2-\frac{3}{4}\left(\frac{x-x_\nu}{h}\right)^3 & : \quad -1 < \frac{x-x_\nu}{h} \le 0 \\ 1-\frac{3}{2}\left(\frac{x-x_\nu}{h}\right)^2+\frac{3}{4}\left(\frac{x-x_\nu}{h}\right)^3 & : \quad 0 < \frac{x-x_\nu}{h} \le 1 \\ \frac{1}{4}\left(2-\frac{x-x_\nu}{h}\right)^3 & : \quad 1 < \frac{x-x_\nu}{h} \le 2 \\ 0 & : \quad \text{else.} \end{cases} \tag{18}$$

The nodes are x_ν and h is the distance between two adjacent nodes. A single spline function is shown in Fig. 5.

In terms of these basis functions the wavefunctions $\varphi_i(x)$ are uniquely defined by a vector of expansion coefficients $a_\nu^{(i)}$

$$\varphi_i(x) = \sum_\nu a_\nu^{(i)} b_\nu(x) \tag{19}$$

and the Hamiltonian is given as a matrix with matrix elements

$$H^{\mathrm{KS}}_{\mu,\nu} = \langle b_\mu | \hat{H}_{\mathrm{KS}} | b_\nu \rangle = \int_{-\infty}^{\infty} dx\, b_\mu(x) \hat{H}_{\mathrm{KS}} b_\nu(x)\,. \tag{20}$$

Since the spline basis is not orthogonal (the overlap of adjacent splines is shown in Fig. 6) the Kohn-Sham equation expressed in this basis is a generalized eigenvalue problem

$$\sum_\nu H^{\mathrm{KS}}_{\mu,\nu} a_\nu^{(i)} = \varepsilon_i \sum_\nu S_{\mu,\nu} a_\nu^{(i)} \tag{21}$$

with an overlap matrix

$$S_{\mu,\nu} = \int_{-\infty}^{\infty} dx\, b_\mu(x) b_\nu(x)\,. \tag{22}$$

This overlap matrix depends only on the basis functions but not on the expansion coefficients. It is therefore suffient to decompose it only once into a lower triangular matrix $\hat{L}$ and its transpose $\hat{L}^{\mathrm{T}}$ using a Cholesky-decomposition[15]. The generalized eigenvalue problem (eq. 21) may then be transformed into a standard eigenvalue problem

$$\left[\hat{L}^{-1}\hat{H}_{\mathrm{KS}}(\hat{L}^{\mathrm{T}})^{-1}\right]\left(\hat{L}^{\mathrm{T}}\vec{a}^{(i)}\right) = \varepsilon_i\left(\hat{L}^{\mathrm{T}}\vec{a}^{(i)}\right) \tag{23}$$

which has to be solved selfconsistently since $\hat{H}_{\mathrm{KS}}$ itself dependes on the density and hence on the solution of the eigenvalue equation.

In each iteration cycle the matrix $\left[\hat{L}^{-1}\hat{H}_{\mathrm{KS}}(\hat{L}^{\mathrm{T}})^{-1}\right]$ is diagonalized numerically using the `zheev` routine from the LAPACK library[16] and the resulting eigenvector $\hat{L}^{\mathrm{T}}\vec{a}^{(i)}$ is transformed back to obtain the eigenvector $\vec{a}^{(i)}$ of the original generalized eigenvalue problem.

The starting point for the selfconsistent scheme is a system of non-interacting particles i.e. a system with $V_{\mathrm{H}} = V_{\mathrm{x}} = 0$. The resulting non-interacting eigenfunctions are then used to construct the first approximation for the Hartee- and the exchange potential and in the subsequent iterations the Hartree- and the exchange potential is calculated from the eigenfunctions of the previous step[22]. To decide whether the iteration has converged we consider the maximum difference between two Kohn-Sham eigenvalues in the n-th and $(n-1)$-th iteration step:

$$\max_i \left|\varepsilon_i^{(n)} - \varepsilon_i^{(n-1)}\right| < \Delta \tag{24}$$

. We found that this difference has to be extremely small compared to the Kohn-Sham eigenvalues themselves which are of the order of several hundred meV, namely $\Delta \approx 10^{-10}$meV. The reason for this very small number are possibly very low lying excitations which correspond to a charge displacement over a large distance in the system. In fact, if Δ is chosen too large, some density range existes where the system seems to be in a delocalized state whereas it is found to be in a localized state if the solution is converged. Generally, to distinguish correctly between a localized and a deloclaized state of the system a high computational accuracy is required.

V. PERSISTENT CURRENT

In this section we discuss the main result of this work. Using the model and the numerical method described in

the previous section we calculated the persistent current in a one-dimensional quantum ring as a function of r_S. Rather than applying the Byers-Yang relation[17] which expresses the persistent current as a derivative of the groundstate energy with respect to the magnetic flux

$$I = -\frac{\partial E}{\partial \Phi} \tag{25}$$

we calculate the current directly from the Kohn-Sham wavefunctions. The obvious advantage is that the Kohn-Sham equations have to be solved only for one specific value of the magnetic flux and no numerical derivative of the ground state energy is required. The total persistent current which is the sum of the paramagnetic current

$$j_p(x) = -\frac{i\hbar}{2m_0^*}\sum_i \left(\varphi_i^*(x)\frac{d}{dx}\varphi_i(x) - \varphi_i(x)\frac{d}{dx}\varphi_i^*(x)\right) \tag{26}$$

and the diamagnetic current

$$j_d(x) = -\frac{\hbar}{m_0^*}\frac{2\pi}{L}\frac{\Phi}{\Phi_0}n(x)\,. \tag{27}$$

has to be constant throughout the system. This is a direct consequence of the continuity equation for the static case which states that $\frac{d}{dx}j(x) = 0$.

In Fig. 7 the relative persistent current (normalized to the persistent current of a non-interacting system in the presence of a weak Gaussian impurity with $V_0 = 0.001$meV) is shown as function of r_S. For the weakest impurity potential used in our calculations with $V_0 = 0.001$meV (black curve) we observe that the persistent current remains constant up to a critical value $r_S^c \approx 2.05$. For larger values of r_S (corresponding to lower densities) the persistent current drops exponentially. We interpret this transition as the formation and pinning of a Wigner crystal phase at r_S^c. Our value of the critical Wigner-Seitz radius may be compared to the equivalent quantity in a two-dimensional electron gas which has been found to be $r_S^{c,2D} = 37 \pm 5$.[18] This large critical number in 2D is probably due to the shear modulus in the two dimensional electron gas[6,19].

For stronger impurity potentials (which are still weak on the energy scale of the Kohn-Sham eigenvalues but comparable to the internal energy of the crystal[20] that is estimated to be on the order of $2-5$meV) the critical value of the Wigner-Seitz radius is shifted to smaller values and instead of a sharp transition at the critical r_S we find a smooth one. For the largest values of impurity potentials considered in this work (5.0meV and 10.0meV, corresponding to the green and magenta curve in Fig. 7, respectively) there is even no range of r_S where we find free electron gas-like behaviour, i.e. where the persistent current is independent of r_S. The absence of a sharp transition for stronger impurity potentials is due to the breaking of the rotational symmetry by the impurity potential itself which inhibits a phase transition.

The evidence for a Wigner transition and the corresponding critical value of r_S found from calculating the

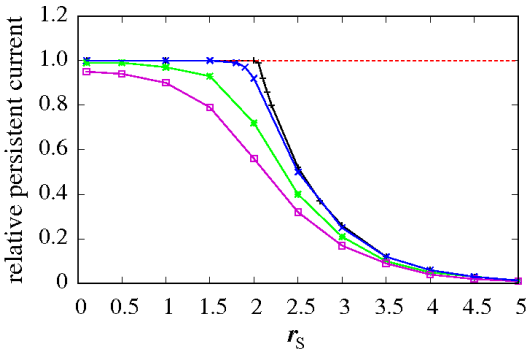

FIG. 7: Relative persistent current as a function of r_S. Colors indicate the unrenormalized strength of the Gaussian impurity potential. Black: 0.001meV, blue: 1.0meV, green: 5.0meV, magenta: 10.0meV. The red dashed line shows the persistent current of a non-interacting system in the presence of a Gaussian impurity with unrenormalized strength 0.001meV.

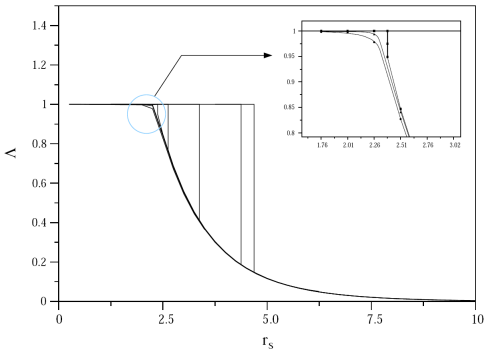

FIG. 8: Curvature of the ground state energy normalized to the non-interacting homogeneous electron gas as a function of r_S. A value of one means delocalization (homogenous electron gas-like behaviour) whereas values smaller than one correspond to increasingly strong localization. Different curves show different impurity potential strength with decreasing disorder from left to right. Taken from Ref. 7

persistent current may be compared to the localization of the one-dimensional electron system as described by the curvature of the groundstate energy[7]. However, in the latter calculation the crystalline phase has been pinned by a random impurity potential rather than by a localized single impurity as in our work. In Fig. 8 a transition to a localized phase is clearly seen. The point of this transition depends strongly on the strength of disorder, that is on the strength of the impurity potential. Despite being not in perfect agreement with our result, the observed critical value of r_S is consistent with our calculations. The deviation is mainly due to the large sensitivity of r_S^c on the strength of the impurity potential.

VI. CONCLUSION

In this work we have studied the persistent current in a one-dimensional quantum ring with ten interacting spinless electrons in the presence of a weak impurity potential. It has been found that the electron electron interacting has a drastic effect on the value of the persistent current. We interpret this result as the formation and pinning of a Wigner crystal phase at a critical value of the one-dimensional Wigner-Seitz radius. However, in our mean-field calculation fluctuations have not been taken into account. We expect therefore that the value of r_S^c we obtained may be underestimated. Furthermore, the dependence of r_S^c on the shape and the width of the pinning potential has not yet been studied. It is thus not yet clear whether our critical value for the one-dimensional Wigner-Seitz radius is universal or not in the sense that it is a property of the interacting one-dimensional electron system alone but does not depend on the precise form of the pinning potential provided that this is weak enough.

I would like to thank Oleg Pankratov for interesting and very stimulating discussions that always provided a deep physical insight into this subject as well as Markus Hofmann who wrote the DFT code used for the calculations.

---

* Electronic address: Siegmund@physik.uni-erlangen.de

[1] T. Ihn, A. Fuhrer, T. Heinzel, K. Ensslin, W. Wegscheider, and M. Bichler, Physica E Low-Dimensional Systems and Nanostructures **16**, 83 (2003).

[2] D. Mailly, C. Chapelier, and A. Benoit, Phys. Rev. Lett. **70**, 2020 (1993).

[3] A. Lorke, R. Johannes Luyken, A. O. Govorov, J. P. Kotthaus, J. M. Garcia, and P. M. Petroff, Phys. Rev. Lett. **84**, 2223 (2000).

[4] E. Wigner, Phys. Rev. **46**, 1002 (1934).

[5] L. Landau and E. Lifschitz, *Lehrbuch der Theoretischen Physik*, vol. V, Statistische Physik Teil 1 (Akademie-Verlag, Berlin, 1979), 5th ed.

[6] L. I. Glazman, I. M. Ruzin, and B. I. Shklovskii, Phys. Rev. B **45**, 8454 (1992).

[7] M. Hofmann, Ph.D. thesis, Universität Erlangen-Nürnberg (2005).

[8] W. Kohn, Phys. Rev. **133**, A171 (1964).

[9] P. Hohenberg and W. Kohn, Phys. Rev. **136**, B864 (1964).

[10] W. Kohn and L. J. Sham, Physical Review **140**, A1133 (1965).

[11] G. Vignale and M. Rasolt, Phys. Rev. B **37**, 10685 (1988).

[12] J. D. Talman and W. F. Shadwick, Phys. Rev. A **14**, 36 (1976).

[13] J. B. Krieger, Y. Li, and G. J. Iafrate, Phys. Rev. A **45**, 101 (1992).

[14] J. B. Krieger, Y. Li, and G. J. Iafrate, Phys. Rev. A **46**, 5453 (1992).

[15] W. H. Press, S. A. Teukolsky, W. T. Vetterling, and B. P. Flannery, *Numerical Recipes in C* (Cambride University Press, Cambridge, 1996).

[16] E. Anderson, Z. Bai, C. Bischof, S. Blackford, J. Demmel, J. Dongarra, J. Du Croz, A. Greenbaum, S. Hammarling, A. McKenney, et al., *LAPACK Users' Guide* (Society for Industrial and Applied Mathematics, Philadelphia, PA, 1999), 3rd ed., ISBN 0-89871-447-8 (paperback).

[17] N. Byers and C. N. Yang, Phys. Rev. Lett. **7**, 46 (1961).

[18] B. Tanatar and D. M. Ceperley, Phys. Rev. B **39**, 5005 (1989).

[19] D. S. Fisher, B. I. Halperin, and R. Morf, Phys. Rev. B **20**, 4692 (1979).

[20] I. V. Krive, P. Sandström, R. I. Shekhter, S. M. Girvin, and M. Jonson, Phys. Rev. B **52**, 16451 (1995).

[21] The xc vector potential is defined analogously to the scalar xc-potential (which is given by $V_{\rm xc} = \frac{\delta E_{\rm xc}[n,\vec{j}_{\rm p}]}{\delta n}$) as a variational derivative of the xc energy with respect to the paramagnetic current density $\vec{A}_{\rm xc} = \frac{\delta E_{\rm xc}[n,\vec{j}_{\rm p}]}{\delta \vec{j}_{\rm p}}$

[22] To ensure convergence the selfconsistent potential in the n-th iteration step is not the full new selfconsistent potential calculated from the density resulting from the previous step. Some fraction of the selfconsistent potential used in the $(n-1)$-th step is linearily mixed to it[7].